Epoxy Nanocomposites Containing Mercaptopropyl Polyhedral Oligomeric Silsesquioxane: Morphology, Thermal Properties, and Toughening Mechanism

Jifang Fu,[1,2] Liyi Shi,[1,2] Yi Chen,[1,2] Shuai Yuan,[1,2] Jun Wu,[2,3] Xinlin Liang,[1,2] Qingdong Zhong[2]

[1]*School of Materials Science and Engineering, Shanghai University, 149 Yanchang Road, Shanghai 200072, People's Republic of China*
[2]*Nano-Science and Nano-Technology Research Center, Shanghai University, Shanghai 200444, People's Republic of China*
[3]*School of Environmental and Chemical Technology, Shanghai University, 149 Yanchang Road, Shanghai 200072, People's Republic of China*

Received 24 June 2007; accepted 26 December 2007
DOI 10.1002/app.27917
Published online 28 March 2008 in Wiley InterScience (www.interscience.wiley.com).

ABSTRACT: A novel polyhedral oligomeric silsesquioxane (POSS) containing a mercaptopropyl group [mercaptopropyl polyhedral oligomeric silsesquioxane (MPOSS)] was synthesized via the hydrolytic condensation of γ-mercaptopropyl triethoxysilane in an ethanol solution catalyzed by concentrated hydrochloric acid and was used to modify epoxy–amine networks by a cocuring reaction with diglycidyl ether of bisphenol A (DGEBA). The structure, morphology, and thermal and mechanical properties of these MPOSS/DGEBA epoxy nanocomposites were studied and investigated with thermogravimetric analysis/differential thermal analysis (TGA–DTA), scanning electron microscopy (SEM), and Fourier transform infrared spectroscopy (FTIR). From SEM analysis, we observed that the miscibility between epoxy and POSS occurred at a relatively high POSS content, which characterized this mixture as a polymer nanocomposite system. The impact test showed that MPOSS reinforced the epoxy effectively, and the SEM study of the impact fracture surface showed that the fibrous yielding phenomenon observed was an indication of the transition of the brittle stage to a ductile stage and correlated well with the large increases in the impact strength; this was in agreement with the *in situ* reinforcing and toughening mechanism. The TGA–DTA analysis indicated that the MPOSS/DGEBA epoxy hybrids exhibited lower thermostability at a lower temperature but higher thermostability and higher efficiency in char formation at an elevated temperature. Differential scanning calorimetry showed that the glass transition temperature (T_g) of the MPOSS/epoxy hybrids were lower than that of the neat epoxy. © 2008 Wiley Periodicals, Inc. J Appl Polym Sci 109: 340–349, 2008

Key words: miscibility; morphology; nanocomposites; reinforcement; polyhedral oligomeric silsesquioxane; thermal properties

INTRODUCTION

Organic–inorganic hybrid polymer nanocomposites have attracted much attention from the polymer community recently. The resulting hybrid nanocomposites, which bear unique properties from both inorganic and organic components, provide a versatile route for controlling the structure and properties of polymers on the nanoscale.[1–5]

Recently, a novel class of organic–inorganic hybrid materials based on polyhedral oligomeric silsesquioxane (POSS) has been developed.[6–11] POSS is an inorganic Si_8O_{12} core, and the core can be designed by the attachment of seven inert organic hydrocarbon groups and a unique functional group or more functional groups that are able to undergo polymerization, grafting, or crosslinking.[12–17] These characteristics offer a chance to prepare hybrid organic–inorganic materials with molecularly dispersed inorganic structural units in nanocomposites. In contrast to clays or conventional fillers, POSS has the advantages of a monodisperse molecular weight with a well-defined structure, low density, high-temperature stability, no trace metals, and sizable interfacial interactions between composite particles and polymer segments. Moreover, when incorporated into a polymer, it provides simplicity in processing and the excellent comprehensive properties of this class of hybrid materials, such as mechanical properties, thermal stability, and flame retardation, thus upgrading properties for numerous high-performance engineering applications.[18–24] Therefore, many nanocomposites with functionalized POSS derivatives with traditional plastics and resins can be designed. It has been reported that monofunctional or multifunctional POSS can be incorporated into the backbone of epoxy resin to improve properties such

Correspondence to: L. Shi (fjfshu@hotmail.com or sly0726@163.com).

Journal of Applied Polymer Science, Vol. 109, 340–349 (2008)

as its thermal properties and reduce flammability properties.[25–34]

The aim of this work was to develop a new kind of mercaptopropyl polyhedral oligomeric silsesquioxane (MPOSS)/diglycidyl ether of bisphenol A (DGEBA) nanocomposite. POSS containing mercaptopropyl (MPOSS) was synthesized and incorporated into DGEBA to form nanocomposites, in which MPOSS was distributed at the molecular level. Thus, it was expected that the properties of the cured DGEBA resin would be improved by the incorporation of MPOSS. In this study, the structure, morphology, and thermal and mechanical properties of these composites were determined with Fourier transform infrared (FTIR) analyses, scanning electron microscopy (SEM), thermogravimetric analysis/differential thermal analysis (TGA–DTA), differential scanning calorimetry (DSC), and so forth.

EXPERIMENTAL

Materials

γ-Mercaptopropyl triethoxysilane [MPTEOS; i.e., $SHCH_2CH_2CH_2Si(OCH_2CH_3)_3$; 98%] was purchased from Shanghai Organosilicon Co. (Shanghai, China). DGEBA [Epoxy 44; epoxy equivalent weight (molecular weight of DGEBA divided by the number of epoxy groups on it) = 213–214 g/equiv] was purchased from Shanghai Resin Co. (Shanghai, China). 3-Methyl-tetrahydrophthalic anhydride (MeTHPA; chemically pure grade) was purchased from Sinopharm Co. (Shanghai, China). MPOSS was prepared in a typical way.[31] Into a flask equipped with a magnetic stirrer, 2.7 mL of deionized water, 20 mL of ethanol, 0.2 mL of concentrated hydrochloric acid (37%), and 23 mL (0.1 mol) of MPTEOS were charged together with an argon blanket. The hydrolysis and rearrangement reactions were carried out, and the mixture was refluxed for 36 h at 60°C to ensure the completion of the hydrosilylation. A viscous liquid was obtained after the removal of the solvent by a reduction of the pressure by a vacuum pump; it was washed with methanol to remove excess MPTEOS and dried in a vacuum oven. Its structure is shown in Scheme 1. A symmetrical polyhedral structure was found through FTIR analysis together with ^{1}H-NMR and ^{29}Si-NMR analyses.

FTIR (KBr, cm^{-1}): 2923, 2858 (alkyl—CH_2—); 2556 (S—H stretching vibration); 1259 (Si—C asymmetric stretching vibration); 1124.91 and 1031.82 (Si—O—Si asymmetric stretching); 694 (Si—C stretching vibration); 572 and 475 (POSS skeletal deformation vibrations). ^{1}HNMR (δ, ppm, $CDCl_3$): 0.78 (double, Si—CH_2—), 1.4 (br, —SH), 1.72 (s, —CH_2—), 2.58 (s, —CH_2—S). ^{29}Si-NMR (δ, ppm, $CDCl_3$): −66.80 (s).

Characterization

The FTIR measurements were conducted on a Nicolet Avatar 320 FTIR spectrometer (Madison, WI) at room temperature in the range of 4000–400 cm^{-1}. MPOSS was granulated, and the powder was mixed with KBr pellets, which were pressed into small flakes. The powder of the cured samples was extracted in chloroform for 2 days to remove the untreated POSS and dried at 150°C before FTIR analysis. ^{29}Si-NMR and ^{1}H-NMR were carried out on a Varian Mercury Plus 400-MHz NMR spectrometer (Palo Alto, CA). The samples were dissolved with deuterated chloroform, and tetramethylsilane was used as the internal reference. A PerkinElmer TGA-7 thermogravimetric analyzer (NETZSCH, Bavaria, Germany) was used to investigate the thermal stability of the nanocomposites. The samples (ca. 10 mg) were heated under the atmosphere from the ambient temperature to 800°C at the heating rate of 10°C/min in all cases. The thermal degradation temperature was taken as the onset temperature at which 5 wt % weight loss occurred. The calorimetric measurement was performed on a PerkinElmer Pyris-1 differential scanning calorimeter (NETZSCH, Bavaria, Germany) in a dry nitrogen atmosphere. All the samples were heated from the ambient temperature to 300°C, and the thermograms were record at a heating rate of 10°C/min. The glass-transition temperatures (T_g's) were taken as the midpoint of the capacity change. A low-voltage scanning electron microscope was used to examine the fracture surface morphology of the samples. To investigate the morphology of POSS-containing epoxy hybrids, the samples were fractured under cryogenic conditions with liquid nitrogen. The fracture surfaces were coated with thin layers of gold of about 100 Å. All specimens were examined with a JSM-6700F scanning electron microscope (JEOL Ltd., Tokyo, Japan) at an activation voltage of 10 kV.

Mechanical property measurements

Mechanical property measurements were taken with impact testing. The no-notch impact strength of the

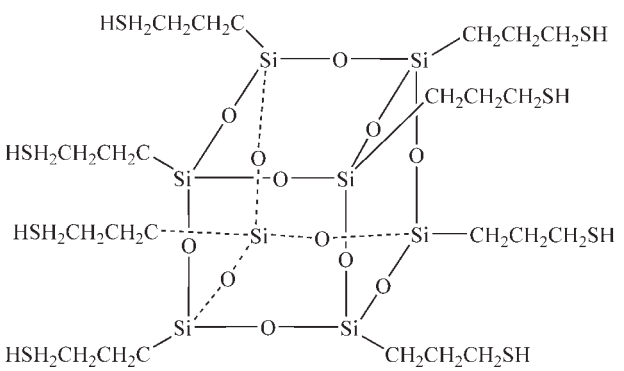

Scheme 1 Chemical structure of MPOSS.

modified epoxy samples was determined with an XJJ-50 Charpy impact tester (Chengde, China) according to China National Standard GB1043-79. The sample size used for the test was 80 × 10 × 4 mm^3. The impact tests were carried out at room temperature. The average value of at least three measurements for each sample was recorded. The impact strength was calculated with the following equation: $\sigma_1 = 1000A/(bh)$, where σ_1, A, b, and h are the impact strength, impact energy, width, and thickness of the sample, respectively.

Preparation of the MPOSS/epoxy nanocomposites

MPOSS/DGEBA composites were made with a solution-blending process. For example, various amounts of MPOSS (amounting to 5, 10, 20, 30, and 40 wt % of DGEBA) and a predetermined amount of DGEBA were dissolved in a little chloroform at 25°C with a magnetic stirrer until homogeneous solutions were obtained; a stoichiometric amount of MeTHPA was then added to the mixtures, and the mixtures were ultrasonicated for half an hour after stirring for half an hour until the systems became transparent and homogeneous. The resulting solutions were poured onto aluminum molds in a vacuum oven (300–350 mmHg) to remove chloroform and gas *in vacuo* at 70°C. The resulting MPOSS/DGEBA hybrids were transparent in each case. The liquid blends were cured at 100°C for 2 h, 150°C for 5 h, and 180°C for 2 h.

RESULTS AND DISCUSSION

Formation of the MPOSS/DGEBA nanocomposites

The hydrosilylation of MPTEOS in the presence of water and concentrated hydrochloric acid as a catalyst and an ethanol solution was employed to synthesize MPOSS. The results of FTIR, ^{1}H-NMR, and ^{29}Si-NMR indicate that MPOSS was successfully obtained. The functional MPOSS was employed to prepare the POSS-containing nanocomposites. The MPOSS-containing nanocomposites were prepared via an *in situ* curing reaction of DGEBA, MeTHPA, and MPOSS in the presence of chloroform. MPOSS was completely dissolved in chloroform, and this gave a transparent solution. It was observed that the ternary mixtures mentioned previously were homogeneous in each case. All the cured hybrid composites were transparent, and this indicated that no phase separation occurred at least on a scale more than the wavelength of visible light. The morphology of the POSS-containing DGEBA hybrids was further investigated by means of SEM.

Figures 1 and 2(a–d) present SEM micrographs of the fracture surfaces of the neat epoxy and the hybrids containing 10 or 40 wt % MPOSS frozen under cryogenic conditions with liquid nitrogen. The hybrid composites exhibited featureless morphologies, and no discernable phase separation was observed; this was similar to what was found for the neat epoxy (Fig. 1). Figure 2(b,d) presents magnified SEM micrographs of frozen damage appearing in the samples shown in Figure 2(a,c), respectively. The SEM images in Figure 2(a–d) showed a single phase. This observation suggests that MPOSS took part in the formation of crosslinked networks and was well proportionately dispersed within the matrix on the nanoscale level.

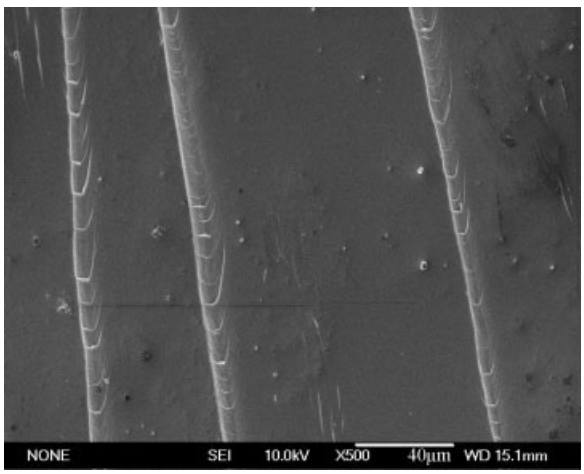

Figure 1 SEM micrograph of the fracture surface of the neat epoxy under cryogenic conditions with liquid nitrogen (500×).

Apart from the curing reaction between DGEBA and MeTHPA, the crosslinking reaction between MPOSS and DGEBA could additionally be involved in the composite system. FTIR spectroscopy was used to examine the degree of the curing reaction after the POSS cages were introduced into the systems. Shown in Figure 3(a,b) are the FTIR spectra of DGEBA, the neat epoxy, and the nanocomposites containing 30 or 40 wt % MPOSS. The pure DGEBA was characterized by the stretching vibration band of epoxide groups at 915 cm^{-1}. In this case, the curing reaction of the neat epoxy (0/100) was quite complete, and this was evidenced by the disappearance of the epoxide band. All the epoxide bands virtually vanished for the POSS-containing nanocomposites under identical curing circles, and this indicated that the curing reactions in the nanocomposites were carried out to completion.[31,33,35] In addition, the DTA curves (shown later in Fig. 8) showed no curing exothermal peaks from the ambient temperature to 350°C, and this further indicated that the curing reaction was quite complete. As discussed in the Experimental section, the FTIR analysis of MPOSS showed Si—O—Si asymmetric stretching peaks at 1124 and 1031 cm^{-1} typical of silsesquioxane cages,

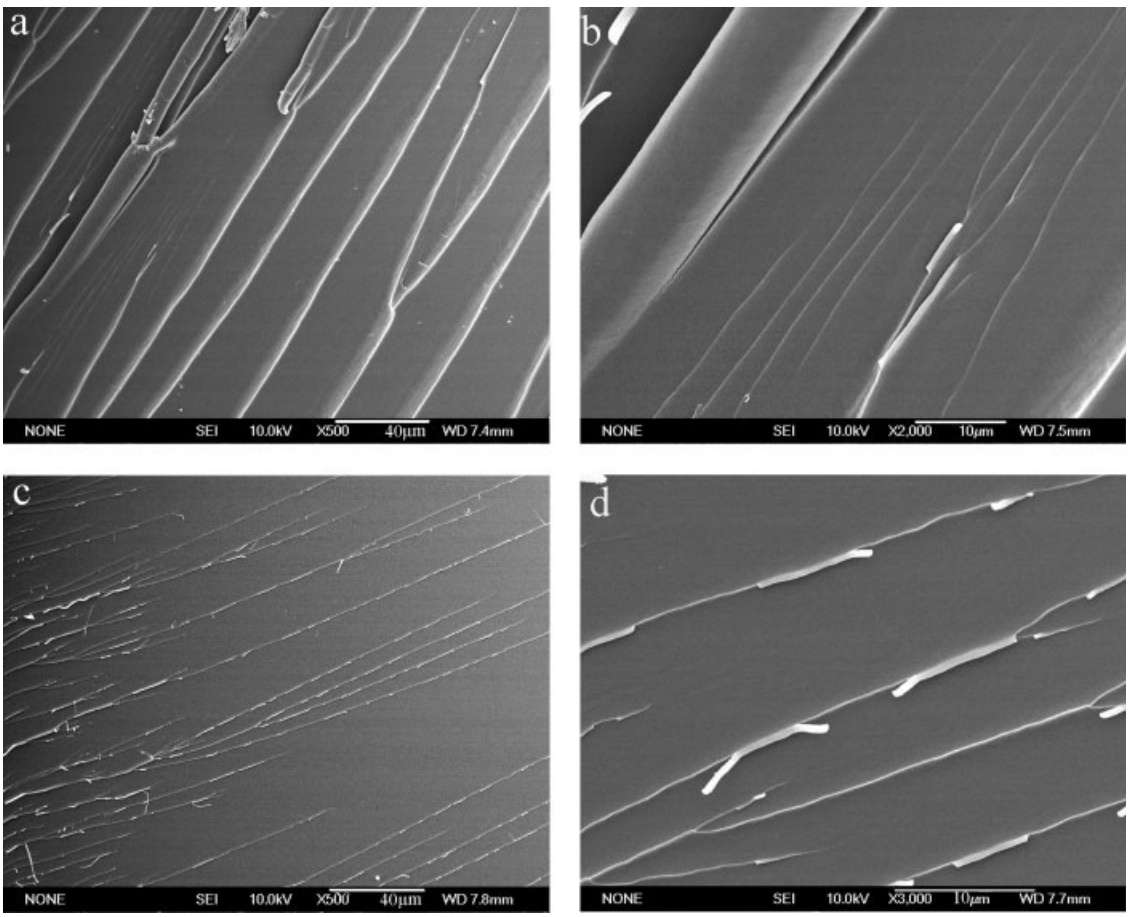

Figure 2 SEM micrographs of the fracture surfaces of the MPOSS hybrids under cryogenic conditions with liquid nitrogen: (a,b) 10% POSS and (c,d) 40% POSS. The magnifications are (a) 500, (b) 2000, (c) 500, and (d) 3000.

a Si—C asymmetric stretching peak at 1259 cm^{-1}, a Si—C stretching vibration at 694 cm^{-1}, and POSS skeletal deformation vibrations at 572 and 475 cm^{-1} together with a —SH stretching vibration at 2556 cm^{-1}.[20,31,34,36] The IR spectrum of MPOSS/DGEBA was very similar to that of the epoxy, except that a sharp and strong Si—O—Si stretching peak appeared at 1128–1034.82 cm^{-1} in all nanocomposites, and other weak characteristic peaks appeared at the low wave numbers. The characteristic peak of —SH at 2556

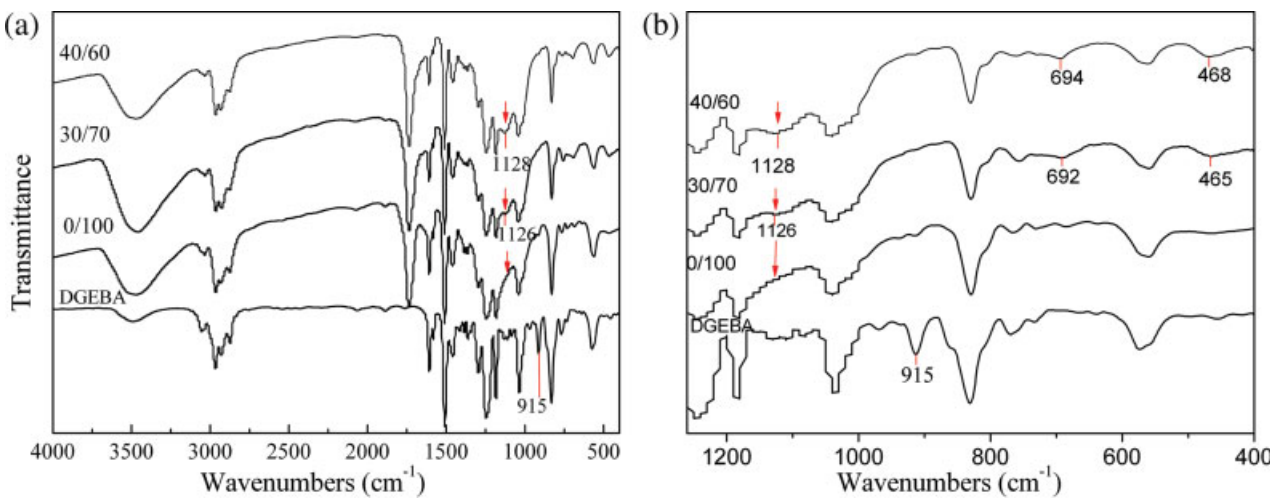

Figure 3 IR spectra recorded at room temperature for uncured pure DGEBA and cured MPOSS/DGEBA nanocomposites (40/60, 30/70, and 0/100 MPOSS/DGEBA). [Color figure can be viewed in the online issue, which is available at www.interscience.wiley.com.]

cm^{-1} is missing in all the spectra of Figure 3. This observation further confirmed that a stronger interaction occurred in the MPOSS/DGEBA polymer hybrids. Figure 3(b) shows expanded spectra of pure DGEBA and various MPOSS/DGEBA hybrids from 1300 to 400 cm^{-1}. The characteristic peaks of MPOSS, such as those at about 1125 cm^{-1} for the Si—O—Si stretching vibration, at 694 cm^{-1} for the Si—C stretching vibration, and at 465 cm^{-1} for the Si—O—Si stretching vibration became stronger with the increase in the MPOSS content. The consistent presence of this Si—O—Si stretching peak confirmed that MPOSS was truly incorporated into the resulting hybrid nanocomposites because the purification procedure for the hybrids ensured the thorough removal of unreacted MPOSS macromers. In terms of the FTIR results, it was judged that in the MPOSS/epoxy hybrids, the epoxy matrices were tightly crosslinked.

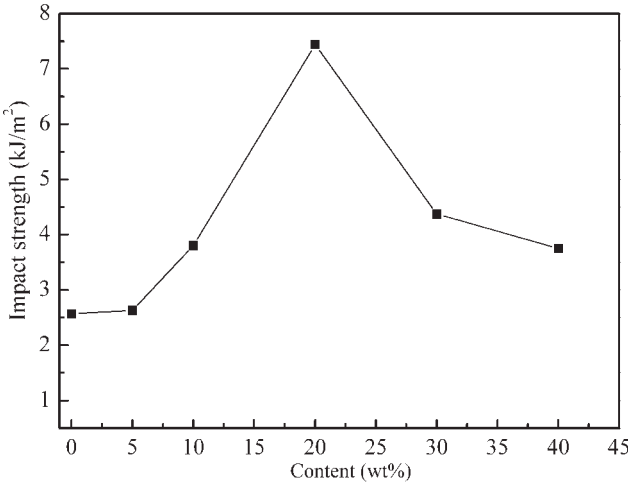

Figure 4 Effect of the content of MPOSS on the impact strength.

Impact strength and toughness mechanism

The effect of the content of MPOSS on the impact strength of the cured DGEBA epoxy resins is shown in Figure 4. It is clear from the figure that the impact strength increased with an increase in the MPOSS concentration, attained a maximum, and then decreased. The maximum impact strength (7.5 kJ/m^2) was achieved at a 20 wt % MPOSS concentration. However, the impact strength of unmodified epoxy was only 2.5 kJ/m^2. The optimum impact strength was about 3 times higher than the value observed for unmodified epoxy. The impact strength improvement of the MPOSS/DGEBA hybrids should be attributed to the miscibility between MPOSS and DGEBA, which could absorb much more energy while impacting.

The impact behavior of the MPOSS/DGEBA hybrids can be explained in terms of the morphology observed with SEM. Scanning electron micrographs of the fracture surfaces are presented in Figure 5. The clear surface and some cracks in Figure 5(a) are substantial evidence of brittle materials. Figure 5(b–d) shows the appearance of a lot of protonema (which refer to a filar shape) with a diameter of about 5 μm for all three cured systems after the cured samples were impacted, which looked like bamboo when they were pulled out.

In the MPOSS/DGEBA hybrid systems, the reaction between the epoxy group of the epoxy resin and the mercapto groups of POSS resulted in excellent miscibility, so there was no phase separation on the fracture surfaces. Therefore, the mechanism of toughness improvement can not be explained by a phase-separation mechanism or anchoring mechanism[29] but can be explained by an *in situ* homogeneous reinforcing and toughening mechanism.[37] The small molecular size of POSS and the reactive group made MPOSS *in situ* disperse homogeneously in the DGEBA matrix, and thus the increased impact performance could also be attributed to the nanoreinforcement effect of POSS cages on the epoxy resin.[35]

In the post yielding process, large amounts of local strain energy were absorbed as the fibrillar microstructure was developed and drawn to high levels of strain in the epoxy matrix. The micrographs clearly show the ductile yielding and fibrillation associated with crack blunting and termination in a hinge-break sample at different levels of magnification. Numerous fibrils observed from SEM suggested that the impact energy had been absorbed.

The findings from the SEM study show that the fibrous yielding phenomenon observed is an indication of the transition of the brittle stage to the ductile stage and correlates well with the large increases of the impact strength. In other words, specimens of high impact strength have more fibrous patterns in the fracture surfaces. This result is in agreement with the findings from a previous work,[38] which also used SEM to analyze fracture surfaces of epoxidized hyperbranched polymer modified DGEBA epoxy. Moreover, similar phenomena and results were also obtained for rubber-toughened poly(vinyl chloride).[39–42]

Thermal properties

Thermal stability

The thermal stability of the MPOSS/DGEBA hybrids was investigated by means of TGA–DTA. Figure 6 shows the TGA thermograms of the epoxy resins containing different concentrations of POSS, which were recorded in the atmosphere at 10°C/min. The corresponding differential thermogravimetry (DTG) curves and DTA curves of these samples are shown in Figures 7 and 8, respectively. In Figure 6, it can

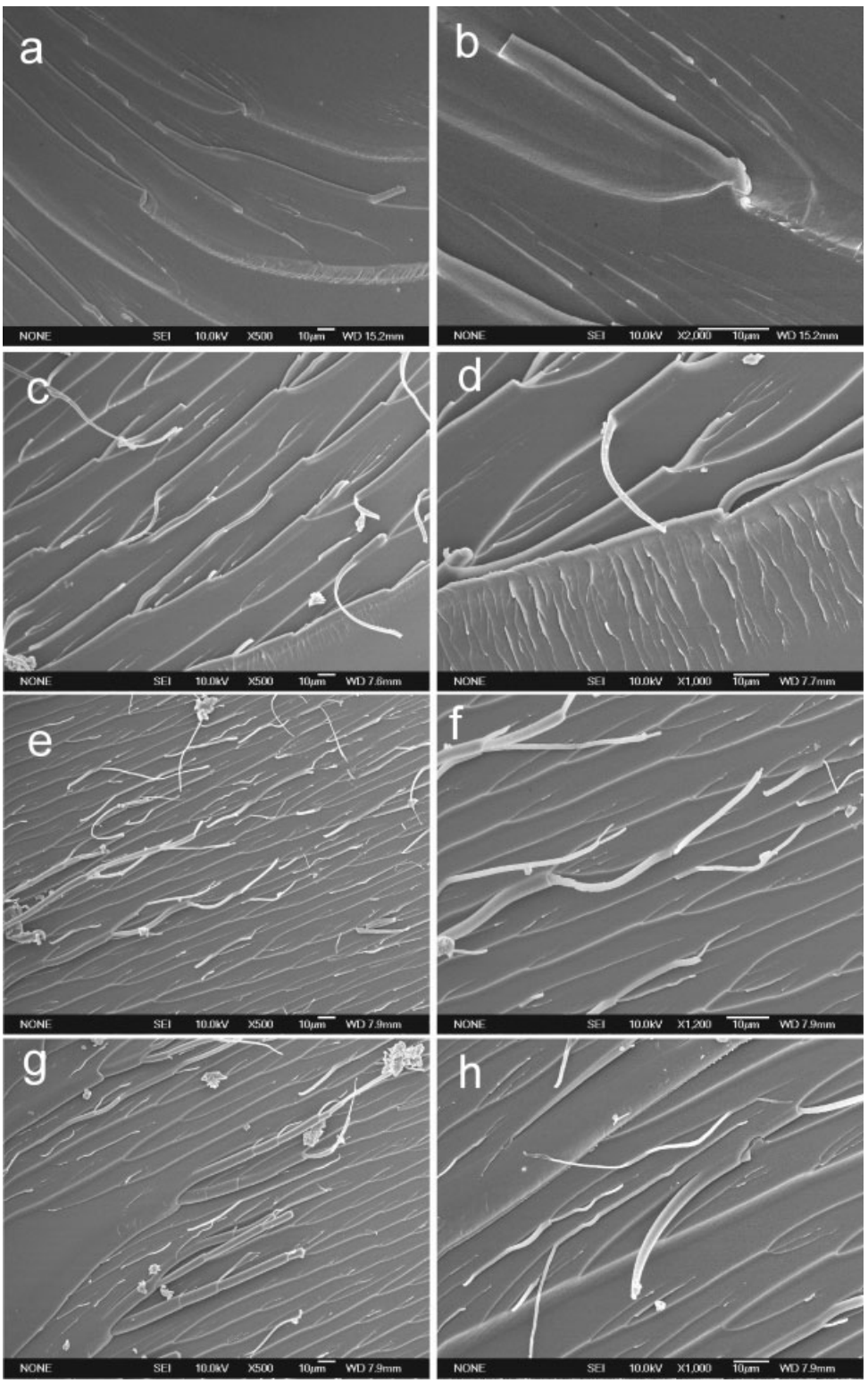

Figure 5 Micrographs of the fracture surfaces of the nanocomposites under impact: (a,b) neat epoxy, (c,d) 10% MPOSS, (e,f) 20% MPOSS, and (g,h) 40% MPOSS. The magnifications are (a) 500, (b) 2000, (c) 500, (d) 1000, (e) 500, (f) 1200, (g) 500, and (h) 1000.

be seen that neat epoxy began to lose weight at about 343°C and degraded almost completely below 760°C. However, MPOSS/DGEBA hybrids still had char yields beyond 800°C, and this suggests that the MPOSS/DGEBA hybrids had higher thermal stability at higher temperatures. MPOSS/DGEBA hybrids containing a higher percentage of MPOSS exhibited lower thermostability at a lower temperature but

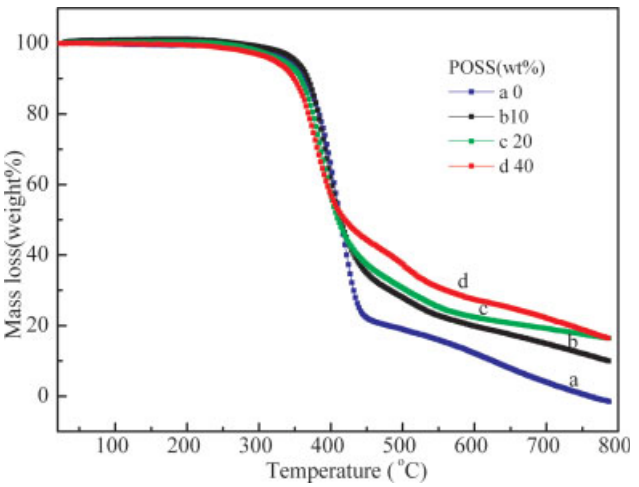

Figure 6 TGA thermograms of POSS/DGEBA hybrids with different contents of POSS: 0, 10, 20, and 40%. [Color figure can be viewed in the online issue, which is available at www.interscience.wiley.com.]

higher thermostability and higher efficiency in char formation at an elevated temperature.

The difference in the degradation behaviors of the MPOSS/DGEBA hybrids can also be seen in the DTG thermograms. On the basis of the number of peaks in the DTG curves, the weight-loss processes of the epoxy resins were divided into several stages. As shown in Figure 7, the DTG curves of the neat epoxy shows two stages corresponding to the degradation of the principal chain of the macromolecule and the oxidation of the carbon chain. However, all the DTG curves of the hybrids show an initial degradation stage at 380–480°C followed by another small stage at the higher temperature of 500°C. The peaks at about 500°C become more obvious and stronger with increasing POSS content. For all the samples, the first maximum is consistent with the first stage of weight loss caused by the pyrolysis of the organic aliphatic unit of the polymer backbone, whereas the second peak is due to the inorganic POSS decomposing, and the third peak is not obvious.

In Figure 8, there are two endothermal peaks at 425–575°C corresponding to the early stage of TGA and an exothermal peak at 570–670°C corresponding to the oxidation loss together with the Si—O condensation in the later stage. The first endothermal peaks shift to the higher temperature with the introduction of POSS, and the second peaks become weak and disappear with the increase in the POSS content. The exothermal peaks shift to a lower temperature with the increase in the POSS content, except for the MPOSS containing 20%. The results are in accordance with the DTG curves and TGA.

The thermal stability factors, including the initial decomposition temperature at which 5% weight loss occurs [T_{IDT} (°C)], apparent decomposition temperature [T_A (°C)], heat-resistant index [T_{zg} (°C)], and temperature at the maximum rate of weight loss [T_{max} (°C)], could be determined from the TGA thermograms.[43,44] In addition, temperatures obtained for mass losses of 10, 15, and 50 wt % (T_{10}, T_{15}, and T_{50}, respectively) were also determined.

T_A (°C) and T_{zg} (°C) were determined by a cut-line (CL) method according to JB2624-79[45] and calculated with the following equations:

$$T_A = (10C - 3B)/7 \quad (1)$$

$$T_{zg} = (T_A + B)/2x \quad (2)$$

where B and C are the temperatures at which 50% weight loss (T_{50}) and 15% weight loss (T_{15}) occur,

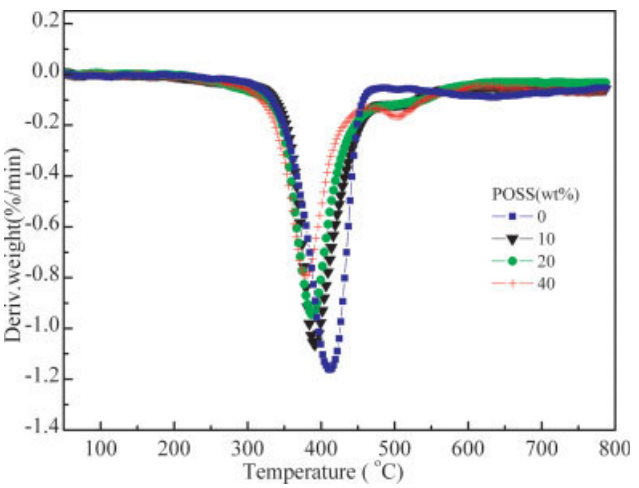

Figure 7 DTG thermograms of POSS/DGEBA hybrids with different contents of POSS: 0, 10, 20, and 40%. [Color figure can be viewed in the online issue, which is available at www.interscience.wiley.com.]

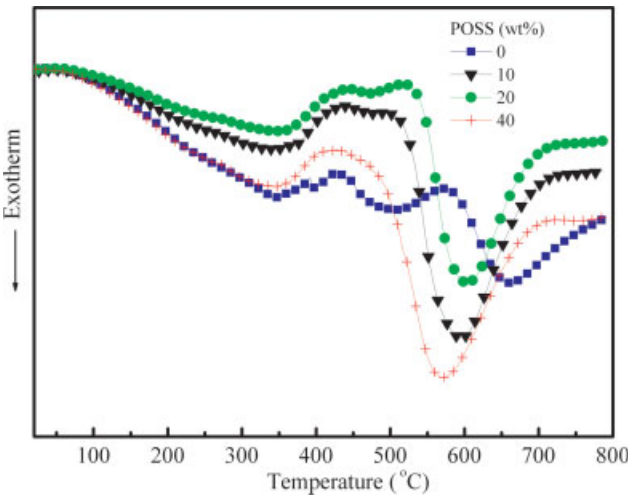

Figure 8 DTA thermograms of POSS/DGEBA hybrids with different contents of POSS: 0, 10, 20, and 40%. [Color figure can be viewed in the online issue, which is available at www.interscience.wiley.com.]

TABLE I
Thermal Stability Factors for MPOSS/DGEBA Hybrids Calculated from TGA Thermograms

POSS (wt %)	T_{IDT} (°C)	T_{10} (°C)	T_{50} (°C)	T_{15} (°C)	T_{max} (°C)	T_A (°C)	T_{zg} (°C)	Char yield (wt %) 500°C	Char yield (wt %) 700°C
0	343.00	364	375.42	413.3	411.9	359.19	162.97	19.0	4.0
10	351.34	368.29	376.8	413.6	391.54	361.03	163.42	27.97	14.90
20	334.14	358.84	368.20	410.37	389.3	350.13	160.44	30.66	19.22
40	323.25	348.8	361.24	419.62	378.31	336.22	159.46	37.40	22.15

respectively, and x is the functionality index. x is 2.37 for the epoxy compounds when the epoxy content is above 50%, and it is 2.14 for the no-epoxy compounds when the epoxy content is below 50%; here it is 2.37.

The results for the thermal stability factors of the hybrids are summarized in Table I.

The values of T_{IDT}, T_A, and T_{zg} increased with the addition of MPOSS first, attained a maximum when the MPOSS content was 10%, and then decreased modestly indeed with the POSS content further increasing. T_{max} decreased slightly for all MPOSS/DGEBA hybrids. This may be explained as follows: an increasing amount of MPOSS decreased the polymer's crosslink density.

The char yield of the hybrids at 500 and 700°C under the atmosphere increased with increasing POSS content, and this indicates that POSS promoted char formation in the MPOSS/DGEBA hybrids. It also indicates that the MPOSS/DGEBA hybrids exhibited lower thermostability at a lower temperature but higher thermostability and higher efficiency in char formation at an elevated temperature. This can be attributed to the yields of silicon-rich residues, which can protect the substrate from heat and flame and thus make the materials more stable at a higher temperature. As a result, POSS influences the degradation behaviors of epoxy resins by self-decomposition and self-condensation at relatively low temperatures, then forming protective layers at higher temperatures and increasing the thermostability.

In conclusion, the epoxy hybrid containing 10% MPOSS presents relatively good thermal stability. This can be mainly attributed to the introduction of POSS into the epoxy network on the nanoscale level and thus the reduction of the diffusion of volatiles in the MPOSS/DGEBA hybrids.[31,33,46,47] MPOSS participated in the formation of the crosslinked network; that is, the POSS was tethered to the polymer matrix. It is possible to propose that mass loss from segmental decomposition via volatiles could be suppressed by well-dispersed POSS cages at the nanoscale. It is also construed as an effect of creating nanocomposites.[36,48] In nanocomposites, tether thermal motion is restricted, and this reduces the organic decomposition pathways accessible to the tether. The inorganic component (POSS) provides additional heat capacity, thereby stabilizing the materials against thermal decomposition. However, when the POSS content increases, the excessive mercaptopropyl groups will compete with the MeTHPA, which will cause the curing agent to be excessive; therefore, there are small molecule in the resin that result in decreasing thermal stability with the great amount of POSS added. Its presence tends to reduce the epoxy crosslinking density. Therefore, the decomposition temperature of the epoxy resin will decrease with increasing POSS content at a concentration. As a POSS structure is thermally degraded, silica and SiO_2 are typically formed to contribute to a higher char yield. Therefore, greater POSS content results in a higher char yield, as would be expected.[34]

Glass-transition behavior

The MPOSS/DGEBA hybrids were subjected to thermal analysis. The DSC curves of the neat epoxy and hybrids are presented in Figure 9. The neat epoxy had a T_g at 101.70°C. Moreover, the MPOSS/DGEBA hybrids displayed slightly lower T_g values than the neat epoxy. Moreover, the hybrids containing 10, 20, or 40 wt % MPOSS had quite close T_g values (98–

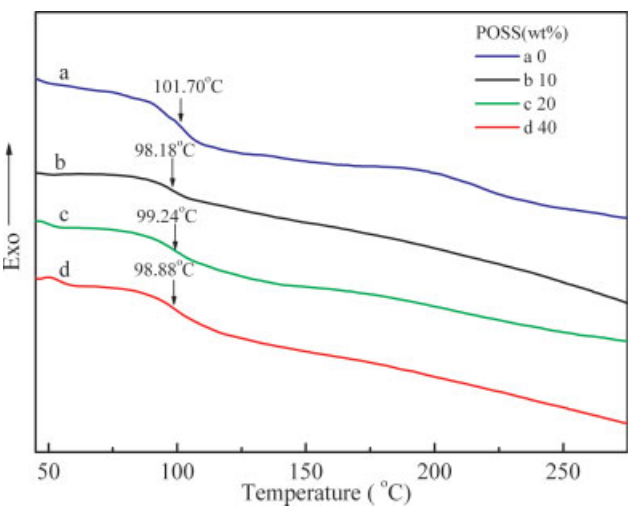

Figure 9 DSC curves of POSS/DGEBA hybrids. [Color figure can be viewed in the online issue, which is available at www.interscience.wiley.com.]

99°C). It appears that the presence of the POSS moiety in the hybrid copolymers was unable to increase the T_g value of the matrix epoxy. In a network structure, T_g is related directly to the crosslinking density.[22] For the FTIR and DTA analysis of cured samples discussed previously, the curing reactions in the hybrids were performed to completion. Therefore, the decrease of T_g could not be ascribed to an incomplete curing reaction. It is proposed that the decrease in T_g could be attributed to the increase in the free volume of the system due to the inclusion of some of the bulky POSS cages on the nanoscale, which is comparable to a plasticization effect.[33]

It has been noted that the effect of POSS cages on T_g of hybrids is dependent on the types of corner R groups on the POSS cages and the interactions between the R groups and matrix polymer.[26] POSS can enhance or reduce T_g of hybrids.

It has been reported that nanocomposites containing POSS display increasing T_g in comparison with the neat polymer, and this has been generally ascribed to the hindering of polymer chain motions of the POSS cages.[15] It has also been found that hybrids containing POSS exhibit decreased T_g values in comparison with the neat polymer, and this is responsible for the increase in the free volume of the system due to the inclusion of some of the bulky POSS cages at the nanoscale level.[33]

Therefore, the two competitive factors mentioned previously determine T_g of the hybrids containing POSS. Obviously, the hindering effect of POSS cages on polymer chain motions will enhance T_g of the hybrids, and the increase in the free volume of the system resulting from the inclusion of the bulky POSS group will decrease T_g of the hybrids. Thus, the behavior of the glass transition of the hybrids containing POSS could be the comprehensive embodiment of the aforementioned factors, depending on the nature of the composite systems. In this case, although the T_g values of the MPOSS/DGEBA epoxy hybrids were lower than that of the neat epoxy, they did not vary significantly with the increase in MPOSS, and this could be attributed to the inhibition effect of POSS cages on molecular motion. This is in marked contrast to the polymer systems plasticized with low-molecular-weight compounds.

The T_g-increase mechanism of POSS/polymer hybrids in ref. 27 seems to fit the results of this study relatively well, and this suggests that the presence of POSS in a smaller amount actually reduces the dipole–dipole interaction of epoxy molecules and plays an inert diluent role, decreasing the self-association interaction of the epoxy matrix; this accounts for the decreasing T_g values for hybrids at a lower loading of POSS. With an increase in the POSS content, T_g of the hybrids increases, and this can be ascribed to the enhancement of the dipole–dipole interaction between the POSS siloxane and the polar groups of the organic polymer.

CONCLUSIONS

In this work, we synthesized MPOSS and used it to modify an epoxy resin to form nanocomposites to study the thermal and mechanical properties, morphologies, and toughening mechanisms. The hybrids were prepared via the cocuring reaction between DGEBA and MPOSS. FTIR analyses provided positive evidence for these types of hydrogen-bonding interactions. From SEM analysis, we observed that the miscibility between DGEBA epoxy and POSS occurred at a relatively high POSS content, which characterized this mixture as a polymer nanocomposite system. The TGA–DTA analysis indicated that the MPOSS/DGEBA hybrids had lower thermostability at a lower temperature but higher thermostability and higher efficiency in char formation at an elevated temperature. DSC showed that the T_g values of the MPOSS/DGEBA hybrids were lower than that of the neat epoxy. The impact test showed that POSS reinforced the epoxy effectively, and the SEM study of the impact fracture surface showed that the fibrous yielding phenomenon observed was an indication of the transition of the brittle stage to the ductile stage and correlated well with the large increases in the impact strength. The toughness mechanism was discussed and was in agreement with an *in situ* reinforcing and toughening mechanism.

References

1. Jose, N. M.; Prado, L. Quim Nova 2005, 28, 281.
2. Sanchez, C.; Lebeau, B.; Chaput, F.; Boilot, J. P. Adv Mater 2003, 15, 1969.
3. Sanchez, C.; Soler-Illia, G.; Ribot, F.; Lalot, T.; Mayer, C. R.; Cabuil, V. Chem Mater 2001, 13, 3061.
4. Shea, K. J.; Loy, D. A. Chem Mater 2001, 13, 3306.
5. Zandi-Zand, R.; Ershad-Langroudi, A.; Rahimi, A. Prog Org Coat 2005, 53, 286.
6. Baker, E. S.; Gidden, J.; Anderson, S. E.; Haddad, T. S.; Bowers, M. T. Nano Lett 2004, 4, 779.
7. Bizet, S.; Galy, J.; Gerard, J. F. Macromolecules 2006, 39, 2574.
8. Cardoen, G.; Coughlin, E. B. Macromolecules 2004, 37, 5123.
9. Chen, Q.; Xu, R. W.; Zhang, J.; Yu, D. S. Macromol Rapid Commun 2005, 26, 1878.
10. Jeon, H. S.; Rameshwaram, J. K. Abstr Pap Am Chem Soc 2003, 226, U528.
11. Joshi, M.; Butola, B. S. J Macromol Sci Polym Rev 2004, 44, 389.
12. Constantopoulos, K.; Clarke, D. J.; Markovic, E.; Uhrig, D.; Clarke, S. R.; Matisons, J. G.; Simon, G. Abstr Pap Am Chem Soc 2004, 227, U441.
13. Lee, A.; Lichtenhan, J. D. Macromolecules 1998, 31, 4970.
14. Lee, J.; Cho, H. J.; Jung, B. J.; Cho, N. S.; Shim, H. K. Macromolecules 2004, 37, 8523.
15. Xu, H. Y.; Kuo, S. W.; Lee, J. S.; Chang, F. C. Polymer 2002, 43, 5117.

16. Zheng, L.; Farris, R. J.; Coughlin, E. B. J Polym Sci Part A: Polym Chem 2001, 39, 2920.
17. Shockey, E. G.; Bolf, A. G.; Jones, P. F.; Schwab, J. J.; Chaffee, K. P.; Haddad, T. S.; Lichtenhan, J. D. Appl Organomet Chem 1999, 13, 311.
18. Yei, D. R.; Kuo, S. W.; Su, Y. C.; Chang, F. C. Polymer 2004, 45, 2633.
19. Pittman, C. U.; Li, G. Z.; Ni, H. L. Macromol Symp 2003, 196, 301.
20. Kuo, S. W.; Lin, H. C.; Huang, W. J.; Huang, C. F.; Chang, F. C. J Polym Sci Part B: Polym Phys 2006, 44, 673.
21. Zhang, Y. D.; Lee, S. H.; Yoonessi, M.; Toghiani, H.; Pittman, C. U. J Inorg Organomet Polym Mater 2007, 17, 159.
22. Lee, Y. J.; Huang, J. M.; Kuo, S. W.; Lu, J. S.; Chang, F. C. Polymer 2005, 46, 173.
23. Zeng, J.; Kumar, S.; Iyer, S.; Schiraldi, D. A.; Gonzalez, R. I. High Perform Polym 2005, 17, 403.
24. Waddon, A. J.; Zheng, L.; Farris, R. J.; Coughlin, E. B. Nano Lett 2002, 2, 1149.
25. Abad, M. J.; Barral, L.; Fasce, D. P.; Williams, R. J. J. Macromolecules 2003, 36, 3128.
26. Dodiuk, H.; Kenig, S.; Blinsky, I.; Dotan, A.; Buchman, A. Int J Adhes Adhes 2005, 25, 211.
27. Xu, H. Y.; Kuo, S. W.; Lee, J. S.; Chang, F. C. Macromolecules 2002, 35, 8788.
28. Huang, J. C.; Xiao, Y.; Mya, K. Y.; Liu, X. M.; He, C. B.; Dai, J.; Siow, Y. P. J Mater Chem 2004, 14, 2858.
29. Kim, G. M.; Qin, H.; Fang, X.; Sun, F. C.; Mather, P. T. J Polym Sci Part B: Polym Phys 2003, 41, 3299.
30. Li, G. Z.; Wang, L. C.; Toghiani, H.; Daulton, T. L.; Koyama, K.; Pittman, C. U. Macromolecules 2001, 34, 8686.
31. Liu, H. Z.; Zheng, S. X.; Nie, K. M. Macromolecules 2005, 38, 5088.
32. Matejka, L.; Strachota, A.; Plestil, J.; Whelan, P.; Steinhart, M.; Slouf, M. Macromolecules 2004, 37, 9449.
33. Ni, Y.; Zheng, S. X.; Nie, K. M. Polymer 2004, 45, 5557.
34. Wang, Y. Z.; Chen, W. Y.; Yang, C. C.; Lin, C. L.; Chang, F. C. J Polym Sci Part B: Polym Phys 2007, 45, 502.
35. Liu, Y. H.; Zheng, S. X.; Nie, K. M. Polymer 2005, 46, 12016.
36. Choi, J.; Kim, S. G.; Harcup, J.; Albert, F. J Am Chem Soc 2004, 123, 11420.
37. Xie, X. L.; Tjong, S. C.; Li, R. K. Y. J Appl Polym Sci 2000, 77, 1975.
38. Zhang, D. H.; Jia, D. M. J Appl Polym Sci 2006, 101, 2504.
39. Calvert, D. J. Ph.D. Thesis, Loughborough University, 1991.
40. Fann, D. M.; Shih, H. Y.; Hsiao, C. M. J Vinyl Technol 1989, 11, 129.
41. Hassan, A.; Haworth, B. J Mater Process Technol 2006, 172, 341.
42. Hiltner, A. S. S. A. Polym Eng Sci 1984, 24, 869.
43. Park, S.-J.; Kim, H.-C.; Lee, H.-I. Macromolecules 2001, 34, 7573 (communication to the editor).
44. Wang, Q. F.; Shi, W. F. Polym Degrad Stab 2006, 91, 1747.
45. Rapid Screening Method of the Thermal Endurance of Insulation Materials by Cut-Line (CL) Method; Standard Method of First Ministry of Machine Building JB2624-79; Technique Standard: Beijing, China, 1979.
46. Sangermano, M.; Malucelli, G.; Bongiovanni, R.; Priola, A.; Harden, A. Polym Int 2005, 54, 917.
47. Liu, H. Z.; Zhang, W.; Zheng, S. X. Polymer 2005, 46, 157.
48. Choi, J.; Kim, S. G.; Laine, R. M. Macromolecules 2004, 37, 99.